# Intermittent Flow of Material and Force-Based Defect Detection During Friction Stir Welding of Aluminum Alloys



Daniel J. Franke, Michael R. Zinn and Frank E. Pfefferkorn

**Abstract** The cost limitations of post-weld inspection have driven the need for in situ process monitoring of subsurface defects. Subsurface defects are believed to be formed due to a breakdown in the intermittent flow of material around the friction stir tool once per revolution. This work examines the intermittent flow of material and its relation to defect formation. In addition, advances have been made in a force-based defect detection model that links changes in process forces to the formation and size of defects. A range of aluminum alloys has been examined, showing that softer aluminum alloys produce less distinct changes in process forces during defect formation and harder aluminum alloys produce more distinct changes when using the same tool geometry.

**Keywords** Aluminum alloys · Nondestructive evaluation Intermittent material flow · Forces

#### Introduction

Friction stir welding (FSW) is a solid-state joining process developed at The Welding Institute in 1991 [1]. During FSW, metallic components are plastically deformed and mechanically intermixed under high pressure and elevated temperature. A significant amount of research has shown that FSW can be used as an energy efficient method of creating high-quality joints in lightweight alloys such as aluminum and magnesium [2–5]. The solid-state nature of this process provides several distinct advantages when compared to fusion welding processes. These advantages include the avoidance of hot cracking, minimal residual stresses and distortion, energy efficiency, and improved joint quality due to grain refinement and minimal thermal effects [2, 3].

D. J. Franke · M. R. Zinn · F. E. Pfefferkorn (☒)
Department of Mechanical Engineering, University of Wisconsin-Madison,
1513 University Ave, Madison, WI, USA
e-mail: frank.pfefferkorn@wisc.edu

Disadvantages of FSW, when compared with fusion welding processes, include large process forces and torques and limitations on weld geometry.

One challenge encountered in the application of the friction stir welding process is the avoidance of sub-surface defects (voids). It is believed that sub-surface defects result from a breakdown in material flow around the probe of the friction stir (FS) tool due to an inadequate thermomechanical state. The thermomechanical state of the process is dependent on a wide range of factors including tool rotational rate, tool traverse rate, FS tool geometry, workpiece material, and thermal boundary conditions. Currently, friction stir welding conditions are empirically determined based on a combination of prior knowledge and trial and error. One goal of this research area is to understand the complex flow around the FS tool probe well enough to accurately simulate and predict defect formation, thus streamlining the application of the process. Additionally, in high-reliability applications, post-weld inspection is often cost prohibitive. Therefore, a secondary goal of this work focuses on developing a real-time in-process defect monitoring system based on a numerical model of the process and measured process output (i.e., a cyber-physical system).

The basis of this work focuses on the intermittent flow of material around the FS tool (specifically the probe) during friction stir welding. Ever since the late 1990s, researchers [6–14] have shown evidence of an intermittent extrusion of material around the FS tool probe once per tool revolution during the friction stir welding of low melting temperature alloys. The most direct evidence of this layer-by-layer transfer is the banded microstructure (Fig. 1) that is often observed in the plane of welding. Figure 1 shows this structure within the region of the stir zone driven by the probe: i.e., 2.5 mm below the workpiece surface. The transverse cross section of the banded microstructure is what produces the prominent features referred to as "onion rings" in friction stir welding literature.

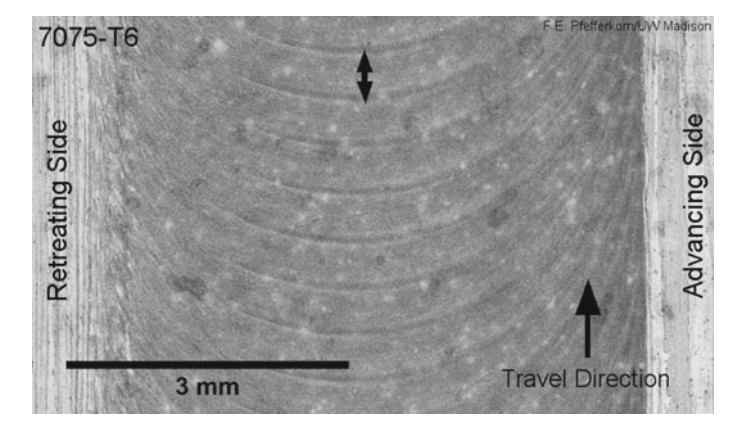


Fig. 1 A reflected light image of the banded microstructure observed in the probe driven region on the stir zone. The double-sided arrow designates the distance the tool travels in one rotation

The underlying physics of how these banded lamellae are formed is a fundamental and unanswered question in the friction stir welding research community. Schmidt et al. [14] and Tongne et al. [15] have both proposed that it stems from a change in contact condition between the tool and workpiece: a change from sticking to sliding or partial sticking/sliding once per tool revolution. Fonda et al. [12] proposed that it stems from a combination of tool runout as well as periodic deflection of the tool (due to the large process forces) once per revolution. Boldsaikhan et al. [16] proposed that a cavity opens up in the wake of the tool probe and is filled in once per tool revolution. Under good welding conditions this cavity is completely filled, and under inadequate conditions, the cavity is not completely filled leaving defects (voids, discontinuities). The most important aspect of the intermittent flow is that several researchers [13, 16–18] have either proposed or shown evidence that the formation of sub-surface defects is directly related to a breakdown of the intermittent flow. This is best exemplified in Fig. 2 which clearly shows the incomplete extrusion of material at a distance equal to the distance the tool moves in one revolution. Therefore, to fully understand sub-surface defect formation mechanisms, the intermittent flow of material must be understood.

Researchers have also linked the intermittent flow of material once per revolution to the oscillation of process forces once per tool revolution. When measuring welding forces in the direction of welding or perpendicular to the direction of welding at a sampling frequency sufficiently greater than the tool rotational frequency, it is evident

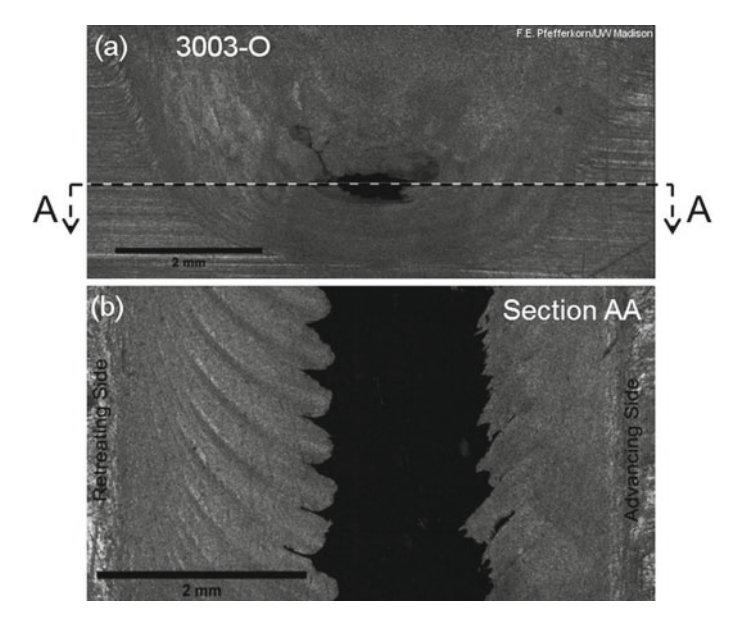


Fig. 2 Reflected light images of a transverse cross section of b section view in the plane of welding showing the incomplete extrusion of material once per tool revolution resulting in the formation of a void

that the forces tend to oscillate at the tool rotational frequency during friction stir welding. This concept was utilized by Boldsaikhan et al. [17] to develop a forcebased method of monitoring weld quality by means of examining the welding forces in the frequency domain. Furthermore, Boldsaikhan et al. [18] developed a heuristic 2D force model that relates the oscillating process forces to the movement of a plasticized shear layer of material that is periodically extruded. Shrivastava et al. [19] built on the work by Boldsaikan et al. by examining the frequency content of the welding forces in depth and provided a physical explanation of what causes changes in process forces during defect formation. The work by Shrivastava et al. utilized the oscillating nature of the process forces to develop a force-based defect detection method that relies on interactions between features on the FS tool and void volumes to produce changes in the process forces. In good welding conditions, the forces in the plane of welding oscillate almost purely sinusoidally as shown in Fig. 3a. This is characteristic of smooth and complete extrusion of material around the FS tool probe once per tool revolution. When examining the force signal in the frequency domain, there is only a significant amplitude at the tool rotational frequency. When using a tool with features on the probe (in this case flats were used), an interaction between the features and the formation of a defect can be captured in the force signal. In the frequency domain, this interaction manifests itself as an amplitude at the harmonic of the tool rotational frequency corresponding to the number of flats on the FS tool probe, e.g., a three flat tool will produce an amplitude at the third harmonic of the tool rotational frequency as shown in Fig. 3b. The amplitude of the third harmonic was correlated to void volume in aluminum alloy 60661-T6 showing good initial agreement. The present study seeks to be a continuation of this method by extending it to other aluminum alloys. This work examines the oscillation of forces in an attempt to further uncover the mechanisms of intermittent flow of material as well as examining how disturbances in the force signals can be used to develop

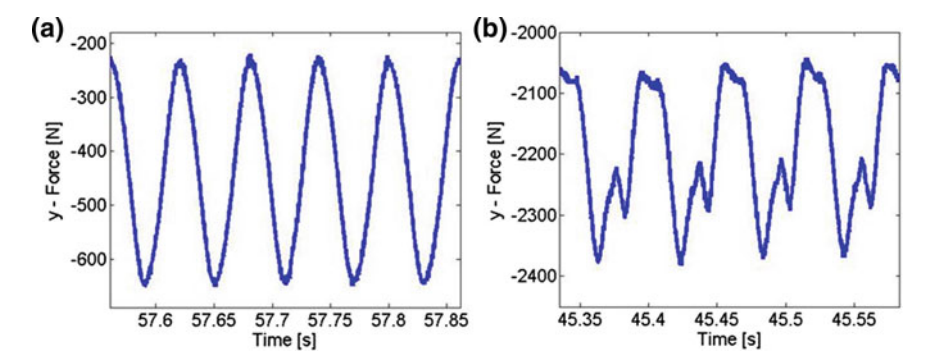


Fig. 3 Measured force signals in the direction of welding in **a** a fully consolidated weld and **b** a weld containing sub-surface defects. Welds were performed in 6061-T6 with a FS tool with three flats on the probe

means of force—measurement-based defect monitoring of the process across different aluminum alloys.

# **Experimental Methods**

Welding was performed on a three-Axis CNC mill (HAAS TM-1). The stiffness of this machine, due to z-axis (plunge) forces, was estimated to be 0.05 mm/kN [20]. Workpieces were mounted on a three-axis piezoelectric force dynamometer (Kistler model 9265). The Dynamometer measures the net force (in each respective direction) that the tool applies to the workpiece. This net force is what is reported in this study. Charge signals from the dynamometer were fed to the charge amplifiers. Outputs from the charge amplifiers were connected to the DAQ system (National Instruments, LabVIEW).

An FS tool made of heat treated H13 tool steel was utilized in this study. It consisted of a concave shoulder with a diameter of 11.6 mm and a threaded, conical probe with three flats. The probe diameter tapered from 7 to 5 mm and was 5 mm in length. All welds were performed with a 3° travel angle. A defined preload was applied to a precision-ground gage block positioned between the trailing edge of the FS tool shoulder and the workpiece in order to establish a consistent plunge depth among welds. This study examined the force signals during defect formation of four different aluminum alloys: 3003-O, 6061-T6, 7075-T6, and 2024-T3. All workpieces were 203 mm (8 in.) long, 102 mm (4 in.) wide and 6.35 mm (0.25 in.) thick. Welding spindle speed was held constant at 1,000 rpm and travel speed was varied between 500 and 600 mm/min. Two replications at both conditions were performed in all four alloys. All welds were 150-mm-long (5.9 in.). Different commanded shoulder plunge depths (specified at the center of the tool) were used in each aluminum alloy in an attempt to produce consistent plunge depths: i.e., position of trailing edge of FS tool shoulder below the workpiece surface. Since the system is compliant, the stiffer and stronger alloys deflect the system more and require a larger commanded shoulder plunge depth to achieve a consistent resultant plunge depth. The commanded plunge depths in the different alloys are listed in Table 1. Material properties believed to

 $\textbf{Table 1} \ \ \text{List of commanded plunge depths for each specific alloy along with material properties taken from MatWeb [21]}$ 

Alloy	Commanded shoulder plunge (mm)	Modulus, E (GPa)	Yield strength (MPa)	Yield strength at temperature (MPa) (°C)
3003-О	0.150	68.9	41.4	12.0 @ 400
6061-T6	0.175	68.9	276	12.0 @ 371
7075-T6	0.525	71.7	503	32.0 @ 371
2024-T3	0.550	73.1	345	28.0 @ 371

be relevant to the plunge depth are also listed in Table 1. The stiffer/stronger alloys produced larger welding forces that generated more deflection in the system. Cross-sectional samples were cut from each weld (25 mm from the end of the weld), polished, and etched. Aluminum alloys 7075-T6 and 2024-T3 were etched with Keller's reagent, whereas 3003-O and 6061-T6 were etched in a modified Poulton's reagent with additional  $HNO_3$ .

## **Results and Discussion**

The goal of this work is to examine the application of the force-based defection method developed in 6061-T6 by Shrivastava et al. [19] on different aluminum alloys. This study friction stir welds four different alloys with the same FS tool using the same processing parameters. The parameters were selected to produces defects in all of the alloys so that the change in the process forces in each alloy can be compared (1,000 rpm and 600 mm/min). Figure 4 shows the cross section of a 3003-O sample with the corresponding force data for three rotations of the tool in the region of

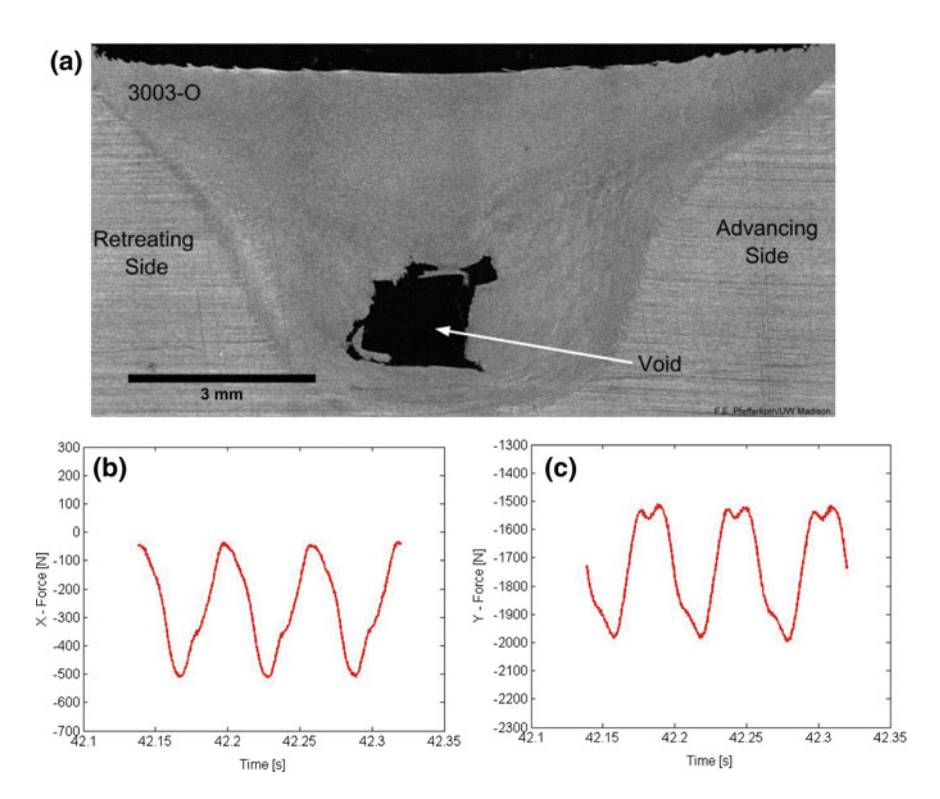


Fig. 4 Results of weld at 1,000 rpm and 600 mm/min in alloy 3003-O: **a** cross section of weld, **b** force signal perpendicular to welding direction, **c** force signal in direction of welding

the weld where the sample was cut from. The Y-direction corresponds to the travel direction of the weld and the X-direction corresponds to the direction in the plane of the workpiece that is perpendicular to the travel direction. A negative Y-direction corresponds to the direction of travel, i.e., the tool will apply an average negative Y-force to the workpiece since the workpiece is resisting the motion of the tool. The negative X-direction corresponds to a force pointing toward the retreating side of the process. Figures 5 through 7 are the corresponding cross sections and force signals for a sample of 6061-T6, 7075-T6, and 2024-T3, respectively. Each force plot shows the time period equal to three rotations of the tool.

Considering that it is not a structural aluminum alloy, 3003-O is the softest and weakest alloy of the four evaluated in this study. The intermediate alloy in this set is 6061-T6, with moderate hardness and hot strength compared to the rest. The two structural alloys, 7075-T6 and 2024-T3, are significantly harder and have a higher hot strength than 3003-O and 6061-T6. These properties govern how the material flows during welding, and how the forces are altered during defect formation. When examining 3003-O, it is clear that the largest defect was produced at these particular welding conditions when compared to the other alloys. It is hypothesized that this occurrence is due to the wide layer of sheared material near the surface of the weld

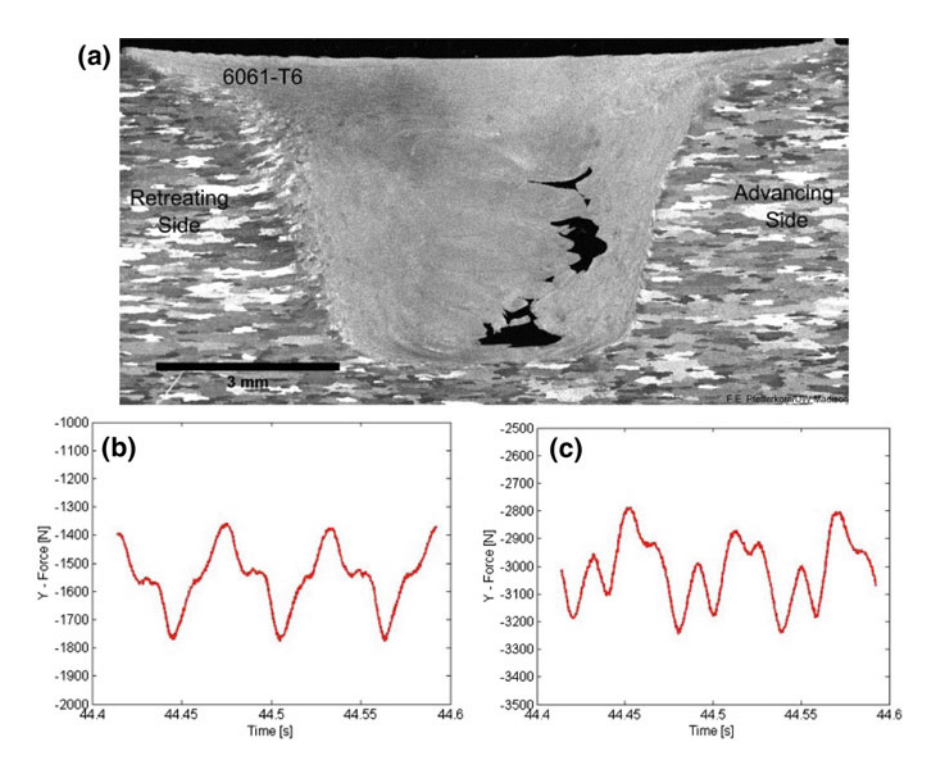
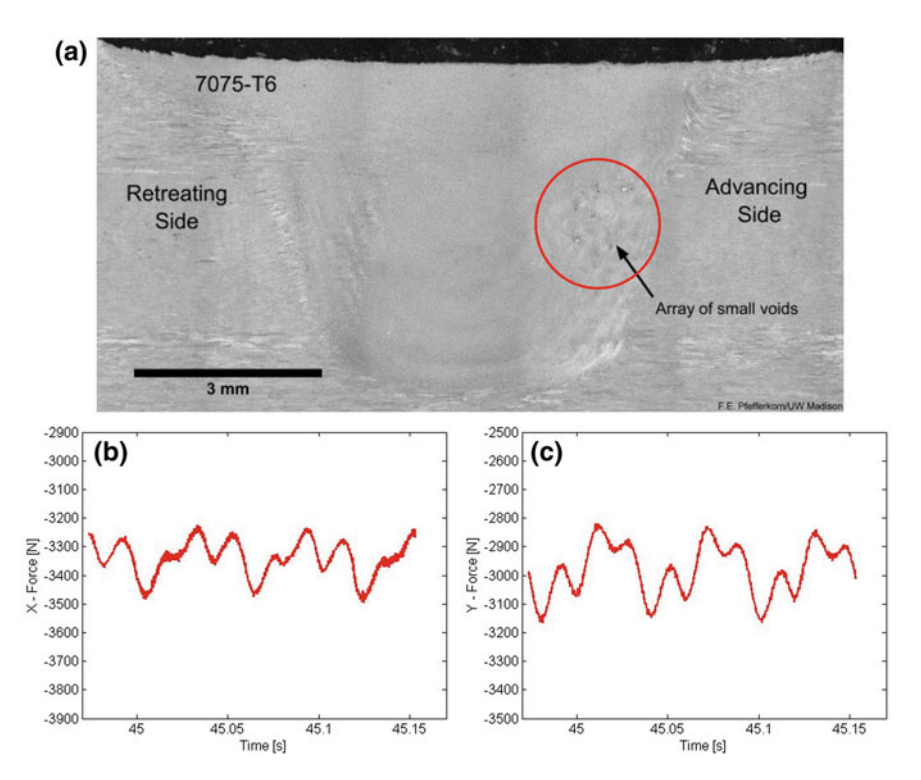


Fig. 5 Results of weld at 1,000 rpm and 600 mm/min in alloy 6061-T6: a cross section of weld, b force signal perpendicular to welding direction, c force signal in direction of welding



**Fig. 6** Results of weld at 1,000 rpm and 600 mm/min in alloy 7075-T6: **a** cross section of weld, **b** force signal perpendicular to welding direction, **c** force signal in direction of welding

(shoulder), which allows the plasticized material to flow up around the shoulder and escape the probe driven region of the stir zone instead of being held and consolidated in the weld. In an application of FSW in 3003-O, an FS tool with a wider shoulder should be used. A larger ratio of the shoulder diameter to probe diameter will allow the shoulder to trap more of the plasticized material generated by the probe. When looking at the harder alloys (2024-T3 and 7075-T6) the stir zone is narrow near the shoulder suggesting that it was harder for material to escape from the weld zone, resulting in smaller defect volumes.

In the study performed by Shrivastava et al. [19] in 6061-T6, larger void sizes correlated with larger amplitudes of the higher harmonic. Interestingly, the 3003-O sample, which has the largest void size, experiences the smallest disturbance in the force signals at the higher harmonic (Fig. 4b, c) when compared to the other alloys tested at the same weld parameters. When examining the harder alloys, even at relatively small void sizes, there is a much more pronounced harmonic. The values of the amplitudes of the force signals at the tool rotational frequency (fundamental frequency) and the third harmonic were extracted from the signals using a discrete Fourier transform, and are reported alongside the average force in Table 2. It is

observed that the larger amplitude values of the third harmonic appear to correlate with a larger average force of the harder and stronger alloys. This makes physical sense because there should be a drop in the oscillatory portion of the force when the void is opening up in the weld since the absence of material will lead to an absence of pressure between the tool and workpiece material. It is hypothesized that at a higher average force the sudden change in force will appear more drastic.

Additionally, in all welds performed in this study, it was observed that the location of the defects within the stir zone was consistent with the phase of the force transients for each particular alloy. In 3003-O the voids reside from the centerline of the weld toward the retreating side, in 6061-T6 they reside halfway between the center of the weld and the advancing side edge, and in 2024-T3 they reside all the way at the advancing side edge of the weld (refer to Figs. 4, 5, and 7). This appears to match the phase of the resultant harmonic in relation to the fundamental amplitude. Figure 8 shows the force signals for the three alloys previously mentioned. In Fig. 8, the location of the harmonic (red line) is done by identifying where the force signal deviates from an ideal sinusoid in the region between the large peaks (blue lines). The red lines are located where the force signal begins to decrease even though a sinusoid should be increasing at this location. As can be seen, it appears that phase of the harmonic shifts in accordance to the location of the void within the stir zone. In 3003-O the harmonic is closer to the left-hand side fundamental peak (void closer to the retreating side of weld), in 6061-T6 the harmonic shifts closer to the righthand side peak (void closer towards advancing side), and in 2024-T3 the harmonic is closest to the right-hand side peak (void all the way towards advancing side). This bolsters confidence that the force oscillation is directly related to the movement of material and that the disruption in the force signal is due to an interaction with the void volume.

## **Conclusions**

The same method of force-based defect detection previously developed for 6061-T6 cannot be directly applied to other aluminum alloys. The disruptions in the force signals at higher harmonics due to interactions with features on the FS tool probe and voids are dependent on the hardness and strength of the alloy. Therefore, a unique approach is required for each alloy.

- For soft alloys, the disruption in the force signal is less pronounced, leading to the challenge of producing good correlations between the harmonic and void size. There is potential to overcome this challenge by using more distinct features on the FS tool probe to produce a more distinct disturbance.
- In harder alloys, there are significant disturbances in the force signal at very small void sizes, or even in fully consolidated welds. This presents the challenge of differentiating between fully consolidated and defective welds.

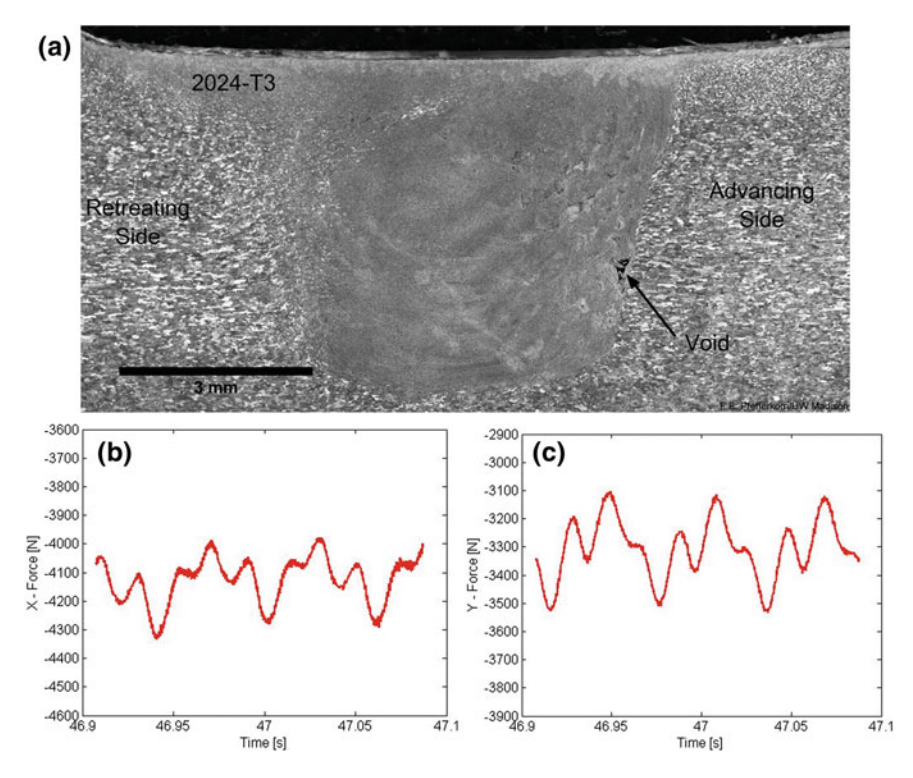


Fig. 7 Results of weld at 1,000 rpm and 600 mm/min in alloy 2024-T3: a cross section of weld, b force signal perpendicular to welding direction, c force signal in direction of welding

**Table 2** Average force values as well as amplitudes at the tool rotational frequency and third harmonic derived using a discrete Fourier transform from the force signals shown in Figs. 4, 5, 6, 7

	3003-O			6061-T6		
	Average	Amp. fun- damental	Amp. third harmonic	Average	Amp. fun- damental	Amp. third harmonic
X-Force (N)	1,710	230	40	3,010	130	80
Y-Force (N)	240	210	30	1,550	140	50
	7075-T6			2024-T3		
	Average	Amp. fun- damental	Amp. third harmonic	Average	Amp. fun- damental	Amp. third harmonic
X-Force (N)	3,440	130	70	2,940	120	70
				1	i e	1

• The same friction stir tool design would not be used to optimally weld the four aluminum alloys used in this study because of their significantly different material flow characteristics. Therefore, future studies should use tools that are better suited for each alloy.

The phase of the higher harmonic appears to match the location of the defect within the stir zone across different alloys. This bolsters confidence in the link between oscillations in force signals and the defect formation process.

**Acknowledgements** The authors gratefully acknowledge financial support of this work by the Department of Mechanical Engineering at the University of Wisconsin-Madison, the Machine Tool Technology Research Foundation, and the U.S. National Science Foundation through grants CMMI-1332738 and CMMI-1826104.

#### References

- Thomas WM, Nicholas ED, Needham JC, Murch MG, Temple-Smith P, Dawes CJ (1991) Friction stir butt welding. GB Patent No. 9125978.8
- 2. Mishra RS, Ma ZY (2005) Friction stir welding and processing. Mater Sci Eng R Rep 50:1-78

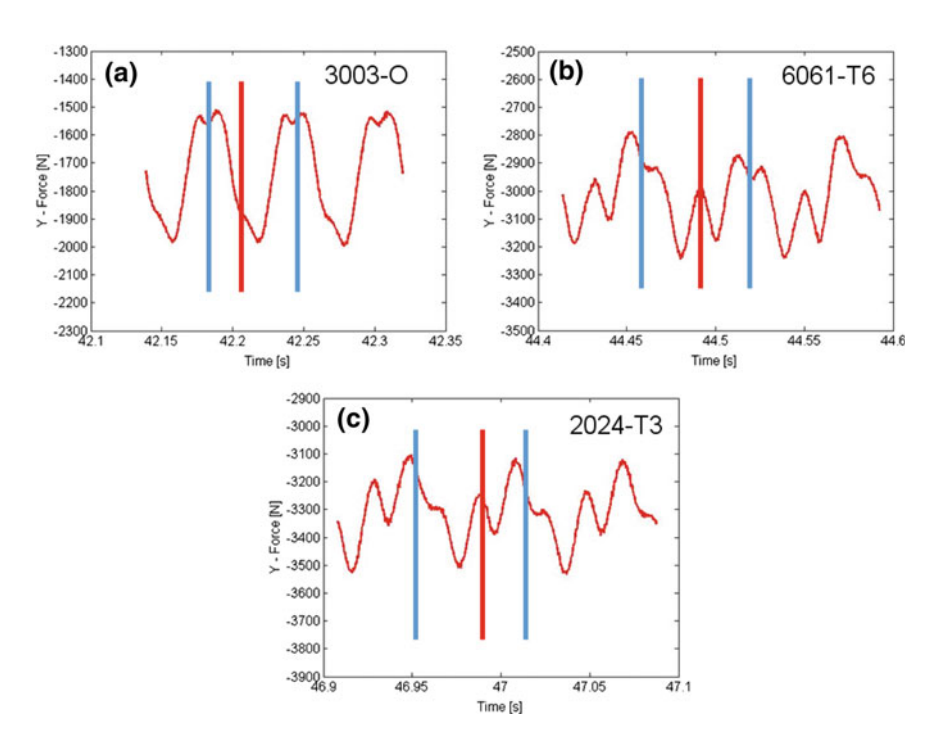


Fig. 8 Force signals in the direction of welding with phase of harmonic identified for a 3003-O, b 6061-T6, and c 2024-T3

- 3. Threadgill PL et al (2009) Friction stir welding of aluminium alloys. Int Mat Rev 54:49–93
- 4. Shrivastava A, Overcash M, Pfefferkorn FE (2015) Prediction of unit process life cycle inventory (UPLCI) energy consumption in a friction stir weld. SME J Manuf Proc 18:46–54
- Shrivastava A, Krones M, Pfefferkorn FE (2015) Comparison of energy consumption and environmental impact of friction stir welding and gas metal arc welding for aluminum. CIRP J Manuf Sci Technol 9:159–168. https://doi.org/10.1016/j.cirpj.2014.10.001
- Krishnan KN (2002) On the formation of onion rings in friction stir welds. Mater Sci Eng A 327:246–251
- Colligan K (1999) Material flow behavior during friction stir welding of aluminum. Weld Res Suppl 229–237
- 8. Kh A, Hassan A, Prangnell PB, Norman AF, Price DA, Williams SW (2003) Effect of welding parameters on nugget zone microstructure and properties in high strength aluminium alloy friction stir welds. Sci Technol Weld Joining 8:257–268
- 9. Prangnell PB, Heason CP (2005) Grain structure formation during friction stir welding observed by the 'stop action technique. Acta Mater 53:3179–3192
- Schneider JA, Nunes AC (2004) Characterization of plastic flow and resulting microtextures in a FSW. Metall Mater Trans B 35(4):777–783
- 11. Arbegast WJ (2003) Modeling friction stir joining as a metalworking process. In: Jin Z (ed) Hot deformation of aluminum alloys III, TMS (The Minerals, Metals, and Materials Society)
- 12. Fonda R, Reynolds A, Feng CR, Knipling K, Rowenhorst D (2013) Material flow in friction stir welds. Metall Mater Trans A 44:337–344
- Abergast WJ (2008) A flow-partitioned deformation zone model for defect formation during friction stir welding. Scr Mater 58:372–376
- Schmidt H, Dickerson TL, Hattel JH (2006) Material flow in butt friction stir welds in AA2024-T3. Acta Mater 54:1199–1209
- Tongne A, Jahazi M, Feulvarch E, Desrayaud C (2015) Banded structures in friction stir welded Al alloys. J Mater Process Technol 221:269–278
- 16. Boldsaikhan E, Burford DA, Gimenez Britos PJ (2011) Effect of plasticized material flow on the tool feedback forces during friction stir welding. Frict Stir Weld Proc VI:335–343
- Boldsaikhan E, Corwin EM, Logar AM, Arbegast WJ (2011) The use of neural network and discrete Fourier transform for real-time evaluation of friction stir welding. Appl Soft Comput 11:4839–4846
- Boldsaikhan E, McCoy M (2013) Analysis of tool feedback forces and material flow during friction stir welding. Frict Stir Weld Proc VII:311–320
- Shrivastava A, Zinn M, Duffie NA, Ferrier NJ, Smith CB, Pfefferkorn FE (2017) Force measurement-based discontinuity detection during friction stir welding. J Manuf Proc 26:113–121
- Shultz EF, Cole EG, Smith CB, Zinn MR, Ferrier NJ, Pfefferkorn FE (2010) Effect of compliance and travel angle on friction stir welding with gaps. J Manuf Sci Eng 132:0410101–0410109
- 21. MatWeb (2018) Material property data. www.matweb.com: Aluminum 3003-O, Aluminum 6061-T6; 6061-T651, Aluminum 7075-T6; 7075-T651, Aluminum 2024-T3